Talanta 109 (2013) 84–90

Contents lists available at SciVerse ScienceDirect

Talanta

journal homepage: www.elsevier.com/locate/talanta

Arsenic and antimony determination in non- and biodegradable materials by hydride generation capacitively coupled plasma microtorch optical emission spectrometry

Alin I. Mihaltan [a], Tiberiu Frentiu [b,*], Michaela Ponta [b], Dorin Petreus [c], Maria Frentiu [a], Eugen Darvasi [b], Constantin Marutoiu [d]

[a] National Institute for Research and Development of Optoelectronics Bucharest, Research Institute for Analytical Instrumentation, Donath 67, 400293 Cluj-Napoca, Romania
[b] Faculty of Chemistry and Chemical Engineering, Babes-Bolyai University, Arany Janos 11, 400028 Cluj-Napoca, Romania
[c] Technical University of Cluj-Napoca, Faculty of Electronics, Telecommunications and Information Technology, Gh. Baritiu 26-28, 400027 Cluj-Napoca, Romania
[d] Faculty of Orthodox Theology, Babes-Bolyai University, Avram Iancu Square 18, 400117 Cluj-Napoca, Romania

ARTICLE INFO

Article history:
Received 25 October 2012
Received in revised form
22 January 2013
Accepted 28 January 2013
Available online 7 February 2013

Keywords:
Arsenic determination
Antimony determination
Recyclable plastic
Biodegradable material
Hydride generation
Capacitively coupled plasma

ABSTRACT

A sensitive method using a miniature analytical system with a capacitively coupled plasma microtorch (25 W, 13.56 MHz, 0.4 l min^{-1} Ar) was developed and evaluated for the determination of As and Sb in recyclable plastics and biodegradable materials by hydride generation optical emission spectrometry. Given their toxicity, As and Sb should be subject to monitoring in such materials despite not being included within the scope of Restriction of Hazardous Substances Directive. The advantages of the proposed approach are better detection limits and lower analysis cost relative to conventional systems based on inductively coupled plasma optical emission and flame atomic absorption spectrometry with/without derivatization. Samples were subjected to acidic microwave-assisted digestion in a nitric–sulfuric acid mixture. Chemical hydride generation with 0.5% $NaBH_4$ after the prereduction of As(V) and Sb(V) with 0.3% L-cysteine in 0.01 mol l^{-1} HCl (10 min contact time at 90 ± 5 °C) was used. Under the optimal hydride generation conditions and analytical system operation the detection limits (mg kg^{-1}) were 0.5 (As) and 0.1 (Sb), whereas the precision was 0.4–7.1% for 10.2–46.2 mg kg^{-1} As and 0.4–3.2% for 7.1–156 mg kg^{-1} Sb. Analysis of two polyethylene CRMs revealed recoveries of 101 ± 2% As and 100 ± 1% Sb.

1. Introduction

Inorganic As compounds have been classified as Group I human carcinogens with variable toxicity depending on the As oxidation state [1]. Although there is no evidence that Sb compounds are carcinogenic, The International Agency for Research on Cancer has characterized antimony trioxide as carcinogenic based on animal testing [2]. For both elements the inorganic compounds of the +3 oxidation state (As(III) and Sb(III)) are more toxic than compounds in +5 oxidation state, As(V) and Sb(V). Antimony in its elemental state is more toxic than its salts. Many inorganic As compounds can be detoxified through methylation in mammals and excreted in urine, unlike Sb compounds. Antimony trioxide is used for its synergistic effect in brominated flame retardants formulations for plastics and is the most important catalyst in the manufacture of polyethylene terephthalate (PET) for water and other beverages bottles. Although As and Sb are not currently listed in the Directives 2002/95/CE and 94/62/CE (Restriction of Hazardous Substances—RoHS), their determination in plastics and biodegradable materials is necessary as they have been listed in the Green Procurement Guidelines by Joint Industry Guidelines. Antimony is also considered a priority pollutant by the U.S. Environmental Protection Agency and the German Research Community [3,4]. Although there are controversial views in the literature on the transfer of Sb compounds from PET in water [5], several studies confirmed the leaching and contamination increase of bottled water upon storage [6–8].

Analytical techniques for Sb determination in plastics include inductively coupled plasma optical emission spectrometry (ICP-OES) and mass spectrometry (ICP-MS) [9,10], flame atomic absorption spectrometry (FAAS) [9,11], energy dispersive X-ray fluorescence (EDXRF) [9] and graphite furnace atomic absorption spectrometry (GFAAS) using slurry or direct solid sampling [12]. The corresponding techniques reported for As determination in plastics are EDXRF [9] and ICP-MS [10]. The development of methods for total content determination and speciation of As and Sb is of increasing interest, as highlighted in several reviews [13–17].

* Corresponding author. Tel.: +40 264 593833; fax: +40 264 590818.
E-mail address: ftibi@chem.ubbcluj.ro (T. Frentiu).

0039-9140/$ - see front matter © 2013 Elsevier B.V. All rights reserved.
http://dx.doi.org/10.1016/j.talanta.2013.01.056

The hydride generation (HG), either chemical or electrochemical, with/without hydride preconcentration is widely used to increase the sensitivity of the determination of As and Sb by spectrometric techniques. Thus HG-AAS [18–20], HG-ICP-OES [21], HG-ICP-MS [22] and atomic fluorescence spectrometry (HG-AFS) [23–25] were mentioned as having improved performance. Recently, the determination of As and Sb has been achieved with good detection limits using HG and detection by miniaturized microwave microstrip plasma optical emission spectrometry (HG-MSP-OES) [26,27] or dielectric barrier discharge atomic absorption or atomic fluorescence spectrometry (HG-DBD-AAS, HG-DBD-AFS) [28–30]. Derivatization by chemical hydride generation involves two steps: prereduction of As(V) and Sb(V) to their species in the +3 oxidation state followed by hydride development in acidic medium with $NaBH_4$ stabilized in alkaline solution. Among agents used to prereduce As(V) and Sb(V) to As(III) and Sb(III), L-cysteine in diluted HCl (0.01–0.03 mol l^{-1}) has proved to be very suitable due to reduction of the contact time and removal of interference in liquid phase [22,31].

The aim of this work was to develop a sensitive method using a miniature analytical system with capacitively coupled plasma microtorch equipped with a microspectrometer to determine As and Sb by hydride generation optical emission spectrometry (HG-μCCP-OES). The possibility of As and Sb determination under similar conditions was investigated using prereduction with L-cysteine and hydride generation in diluted HCl. The optimized conditions for chemical derivatization and plasma operation, and the detection limits relative to other analytical systems are presented. The optimized methodology was applied to recyclable plastics from electronics and packaging containing non- and biodegradable materials and validated by analyzing two polyethylene certified reference samples. The study is of analytical importance given the current interest in the development of simple, low-cost and user-friendly miniature analytical systems for dedicated applications.

2. Experimental

2.1. Instrumentation

The μCCP-OES system had been previously used for the simultaneous multielemental analysis of environmental samples after mineralization and Hg determination in non- and biodegradable materials and water after cold vapor generation [32–34]. The HG-μCCP-OES experimental set-up (Fig. 1) consists of a capacitively coupled plasma microtorch (INCDO-INOE 2000 Bucharest, Research Institute for Analytical Instrumentation, Cluj-Napoca, Romania), free-running generator (13.56 MHz, 10–30 W, $15 \times 17 \times 24$ cm^3) (Technical University of Cluj-Napoca, Romania), HGX-200 hydride generation system (Omaha, Nebraska, USA) and HR 4000 microspectrometer (Ocean Optics, Dunedin, Florida, USA). The optical signal was collected *via* a QP fiber optic (600 μm diameter, 25 cm length) and processed by SpectraSuite software as the average of 10 measurements with a 5 s integration time. The viewing zone in plasma was selected by moving the fiber optic in 0.1 mm increments using an XYZ translator. The hydride generator was coupled with the plasma microtorch using a PTFE tube.

Plasma was developed within a quartz tube (25 mm length, 5 mm i.d. and 160 nm cut-off; H. Baumbach & Co, Ltd., Ipswich Suffolk, UK) on the tip of a 1-mm-diameter Mo microelectrode connected to an RF generator. Hydrides were carried into the plasma by a 0.3–0.5 l min^{-1} Ar flow rate through four 0.75-mm-diameter channels crossing the Mo microelectrode support on a 3-mm-diameter rim.

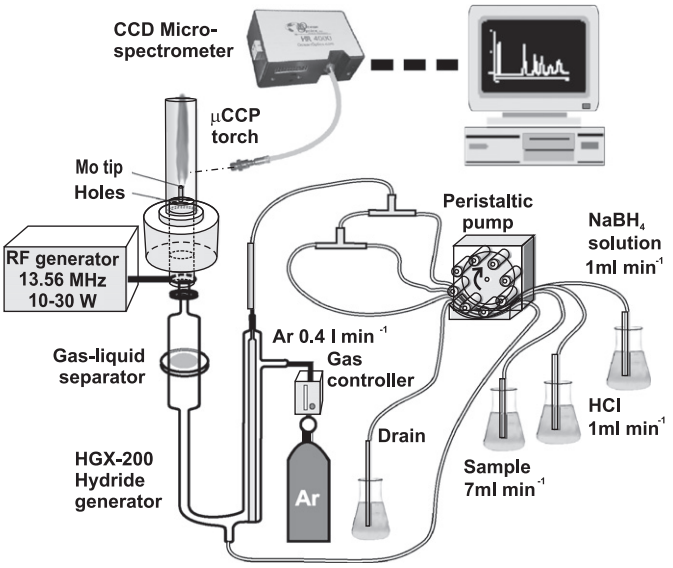

Fig. 1. Schematic of the HG-μCCP-OES set-up.

An MW3S+ Berghof model closed-vessel microwave digestion system (Berghof, Germany) at controlled temperature was used for sample mineralization. The pH of the samples was adjusted to 2.00 ± 0.01 prior to hydride generation using a 540 GLP pH-meter (WTW GmbH, Weilheim, Germany).

2.2. Reagents, standard solutions, CRMs and samples

Hydrochloric acid (10 mol l^{-1}) for As determination (< 5 ng l^{-1} As), $NaBH_4$ (> 96%), NaOH ACS (> 99%) and L-cysteine BioChemika Mikroselect (> 99.5%) purchased from Fluka-Chemie (Buchs, Switzerland) were used. Nitric acid (65%), H_2SO_4 (97%) and stock solutions of 1000 μg ml^{-1} As(V) and Sb(V) were procured from Merck (Darmstadt, Germany). Throughout the study, Milli-Q water obtained in laboratory (Millipore Corp., Bedford, USA) was used. The glassware was soaked in 5 mol l^{-1} HNO_3 for at least 12 h and rinsed with Milli-Q water.

Stock solutions of 10% L-cysteine in 0.005–0.05 mol l^{-1} HCl were prepared. Solutions of 50 ng ml^{-1} As(V) and 10 ng ml^{-1} Sb(V) in 0.005–0.05 mol l^{-1} HCl in the presence of 0.02–0.7% L-cysteine and solutions of 0.005–0.05 mol l^{-1} HCl as a carrier toward the hydride generator were prepared for optimizing the prereduction and derivatization processes. Solutions of 0.2–0.7% $NaBH_4$ stabilized in 0.5% NaOH and solutions containing 0.5% $NaBH_4$ stabilized in 0.2–0.7% NaOH were also prepared for optimizing the hydride generation. Standard solutions of 5–100 ng ml^{-1} As and 1–100 ng ml^{-1} Sb in 0.01 mol l^{-1} HCl in the presence of 0.3% L-cysteine were used to calibrate the HG-μCCP-OES system.

Two polyethylene granule certified reference materials were employed for method validation: ERM-EC 680k and ERM-EC 681k (LGC, Promochem, Wesel, Germany).

The real samples were recyclable plastic based on acrylonitrile-butadiene-styrene copolymer (ABS) from electronic equipment, polyethylene (PE) shopping bags, materials containing oxo-biodegradable polyethylene (OPE) with 98% PE or corn starch for food packaging and polyethylene terephthalate (PET) bottles for still and mineral water.

2.3. Sample treatment

Samples were cut into pieces, washed, air-dried and ground to grain size < 2 mm using a cutting mill. Next, 150 mg samples were subjected to high-pressure (100 atm) microwave digestion

Table 1
Operating conditions for the mineralization of non- and biodegradable materials using the microwave digester.

	Stage				
	1	2	3	4	5
Temperature (°C)	145	170	190	100	100
Hold (min)	5	10	15	10	10
Ramp time (min)	2	2	2	1	1
Power (%)[a]	80	80	80	0	0

[a] 100% power corresponds to 1450 W.

in a mixture of 3 ml of 65% HNO_3 and 3 ml of 97% H_2SO_4 using the protocol presented in Table 1.

A volume of 1.5 ml of 10% L-cysteine in 0.01 mol l^{-1} HCl was added to the digest, and the mixture was heated in a boiling water bath at 90 ± 5 °C for 10 min to prereduce As(V) and Sb(V) to As(III) and Sb(III), respectively. After cooling, the solution was adjusted to 2.00 ± 0.01 pH with NaOH solution by potentiometric measurement and diluted to 50 ml with 0.01 mol l^{-1} HCl. The final concentration of L-cysteine was 0.3%. When the As or Sb concentration in the digest exceeded the calibration range, up to a 10-fold dilution was carried out prior to prereduction. The calibration standards were prepared in the same way as the samples.

A blank calibration solution and two blank test solutions were prepared to establish the measurement scheme and background correction in HG-μCCP-OES. The blank calibration solution contained 0.3% L-cysteine in 0.01 mol l^{-1} HCl, similar to the calibration solutions. One of the blank test contained 1.5 ml of 10% L-cysteine in 0.01 mol l^{-1} HCl, 3 ml of 65% HNO_3 and 3 ml of 97% H_2SO_4 diluted to 50 ml solution with 0.01 mol l^{-1} HCl. The other blank test corresponding to the 10-fold diluted samples contained 1.5 ml of 10% L-cysteine in 0.01 mol l^{-1} HCl, 0.3 ml of 65% HNO_3 and 0.3 ml of 97% H_2SO_4 diluted to 50 ml solution with 0.01 mol l^{-1} HCl.

3. Results and discussion

3.1. Emission spectra of As and Sb and measurement scheme in HG-μCCP-OES

Fig. 2 presents the background emission spectrum of plasma at 0.8 mm and 1.6 mm observation heights for the blank calibration solution and two blank test solutions.

An increase of the continuous background, and a decrease of the molecular emission of NO ($A^2\Sigma^+ \rightarrow X^2\Pi$), OH radical ($A^2\Sigma^+ \rightarrow X^2\Pi$) and N_2 second positive system ($C^3\Pi_u \rightarrow B^3\Sigma_g$) were observed in the presence of H_2 (B,C,D spectra) generated by $NaBH_4$ in acidic medium. In the same time, no difference among the continuous background levels of the three blank solutions was encountered. As a result, the spectrum of the blank calibration solution (0.3% L-cysteine in 0.01 mol l^{-1} HCl) was used as reference for background correction in the further measurements.

The measurement scheme by HG-μCCP-OES involved: (i) record of the spectrum for the blank calibration solution; (ii) background correction and (iii) record of the spectrum for the calibration standards and sample tests. The memory effects in the introduction of samples were removed by washing the sample channel of the HGX-200 system with the blank calibration solution for 40 s.

The emission spectrum for a test solution containing 50 ng ml^{-1} As and Sb recorded following the above scheme is presented in Fig. 3.

The main resonance lines of As (189.042 nm; 193.759 nm; 197.262 nm) were not accessible because of their location outside the spectral range covered by the detector, while the main resonance line of Sb 217.582 nm because of the low sensitivity of the detector at this wavelength. Emission intensity of As and Sb lines is governed by both plasma excitation capability and detector response curve. Thus the alternative lines 228.812 nm for As and 259.805 nm for Sb were selected as they provided the best sensitivity for this spectrometric equipment.

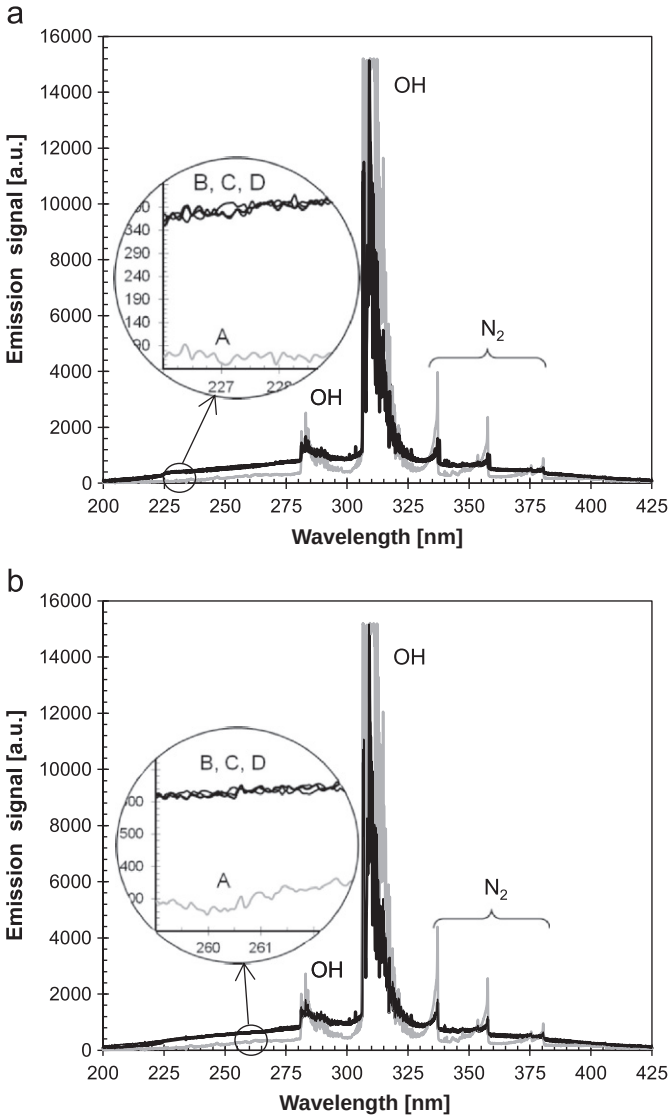

Fig. 2. Background emission spectrum of plasma at 0.8 mm (a) and 1.6 mm (b) observation heights. A—sample channel: water; carrier channel: water; reducing reagent channel: water; B—sample channel: blank calibration solution (0.3% L-cysteine in 0.01 mol l^{-1} HCl); carrier channel: 0.01 mol l^{-1} HCl solution; reducing reagent channel: 0.5% $NaBH_4$ in 0.5% NaOH solution; C—sample channel: blank test solution (1.5 ml of 10% L-cysteine in 0.01 mol l^{-1} HCl, 3 ml of 65% HNO_3 and 3 ml of 97% H_2SO_4 diluted to 50 ml solution with 0.01 mol l^{-1} HCl); carrier channel: 0.01 mol l^{-1} HCl solution; reducing reagent channel: 0.5% $NaBH_4$ in 0.5% NaOH solution; D—sample channel: blank test solution (1.5 ml of 10% L-cysteine in 0.01 mol l^{-1} HCl, 0.3 ml of 65% HNO_3 and 0.3 ml of 97% H_2SO_4 diluted to 50 ml solution with 0.01 mol l^{-1} HCl); carrier channel: 0.01 mol l^{-1} HCl solution; reducing reagent channel: 0.5% $NaBH_4$ in 0.5% NaOH solution. Plasma power: 25 W; Ar flow rate: 0.4 l min^{-1}.

3.2. Optimization of the HG-μCCP-OES parameters

The HG-μCCP-OES working parameters were optimized with respect to hydride generation conditions and Ar plasma operation.

The concentrations of HCl and L-cysteine in the sample, HCl in the carrier, $NaBH_4$ and NaOH in the derivatization reagent were

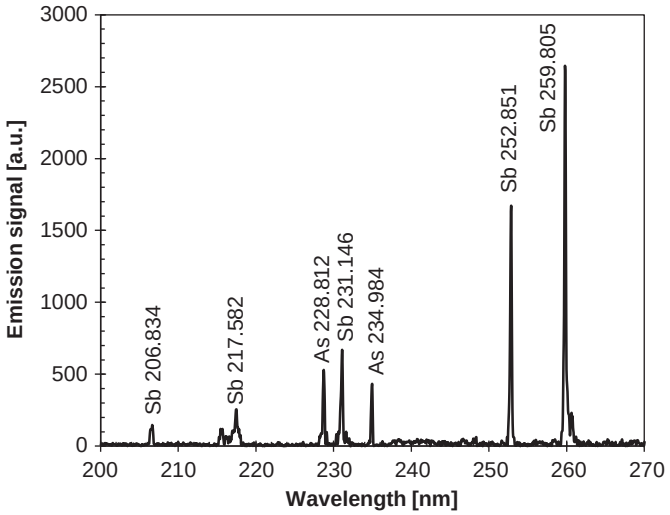

Fig. 3. Emission spectrum of As and Sb in plasma at 25 W and 0.4 l min^{-1} Ar flow rate with a 1.2 mm observation height. Sample test: 50 ng ml^{-1} As and Sb in 0.01 mol l^{-1} HCl and 0.3% L-cysteine. Derivatization reagent: 0.5% $NaBH_4$ stabilized in 0.5% NaOH.

selected to generate the highest emission signal for As and Sb. In a previous study [35], we found that As(V) was completely prereduced to As(III) by 1% L-cysteine in 0.01 mol l^{-1} HCl after heating in a 90 ± 5 °C water bath for 10 min. Feng et al. [22] also reported the complete prereduction of Sb(V) to Sb(III) with 0.3% L-cysteine in 0.03 mol l^{-1} HCl at room temperature within 6–10 min. In this work, the prereduction of As(V) and Sb(V) was achieved according to the procedure previously developed in our laboratory [35]. Volumes of 0.1–3.5 ml of 10% L-cysteine in 0.005–0.05 mol l^{-1} HCl were added to samples containing As(V) and Sb(V) in 0.005–0.05 mol l^{-1} HCl. The resulting solutions were then heated in a 90 ± 5 °C water bath for 10 min and, after cooling, diluted to 50 ml with 0.005–0.05 mol l^{-1} HCl, yielding a final L-cysteine concentration of 0.02–0.7%. In the hydride generation step, the carrier was HCl solution, matching the sample acidity.

Among the parameters investigated for arsine and stibine generation, the HCl concentration was found to be critical in both the sample and the carrier. The experiments indicated a maximum signal with respect to both elements for 0.01 mol l^{-1} HCl in the sample and the need for rigorous pH control in the range of 2.00 ± 0.01. Regarding L-cysteine, its optimum concentration in the sample was 0.2% for As(III) and 0.3% for Sb(III). A sharp increase in the emission signal for both elements was observed as the L-cysteine concentration increased up to 0.1%. In the case of As, there was no significant difference in the emission signals in the presence of 0.2% and 0.3% L-cysteine. Thus, a 0.3% concentration of this reagent was selected for the simultaneous derivatization of As(III) and Sb(III).

The effect of $NaBH_4$ concentration on derivatization efficiency was investigated within the range 0.2–0.7%, and the maximum emission for As was observed for 0.5% $NaBH_4$. For Sb, the emission increased sharply with increasing $NaBH_4$ concentration up to 0.4%, after which the signal slightly decreased. Therefore, a $NaBH_4$ concentration of 0.5% was selected for the derivatization step. The concentration of NaOH as a stabilizer for $NaBH_4$ had the smallest effect on both As and Sb emission, although a slight maximum was observed for 0.5% NaOH.

All subsequent measurements were performed under the following conditions: (i) prereduction with 0.3% L-cysteine in 0.01 mol l^{-1} HCl for 10 min in a 90 ± 5 °C water bath; (ii) rigorous adjustment of sample pH to 2.00 ± 0.01 by potentiometric titration with NaOH after prereduction; (iii) derivatization with 0.5% $NaBH_4$ stabilized in 0.5% NaOH in the presence of 0.3% L-cysteine; and (iv) solution of 0.01 mol l^{-1} HCl as the carrier.

The plasma microtorch was optimized with respect to operating conditions (Ar flow rate and power level) and observation height to achieve the highest emission signal. It was found that the operating conditions were the key to igniting and sustaining a stable plasma, and influenced emission of both background and analyte. The minimal power to sustain our plasma was 10 W. For more than 30 W the diffuse discharge turn into an arc as a result of the overheating of the microelectrode, which is not water cooled. The dissipated power into plasma was adjusted between 20 W and 30 W through the voltage applied to the electrode from the RF generator. Using a class E amplifier provided a yield coupling efficiency of the power of at least 80%. Argon flow rate determines the residence time of the analyte in plasma and thereby the atomization/excitation process of the analyte. Plasma is unstable for Ar flow rate below 0.1 l min^{-1} because of air diffusion. Fig. 4 presents the dependence of emission signal on Ar

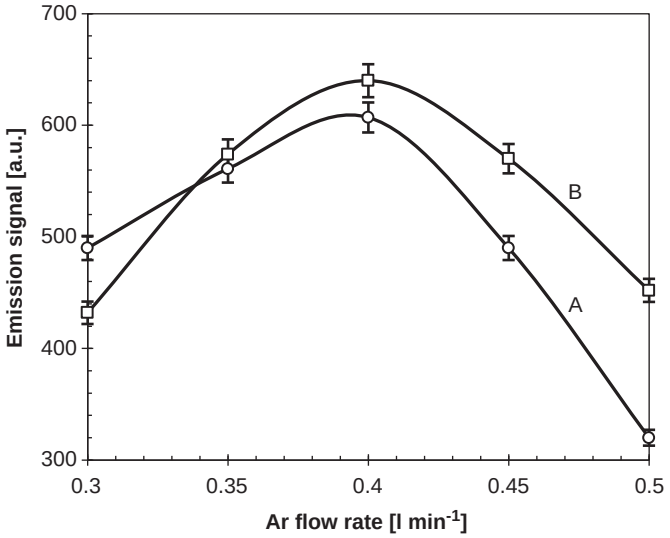

Fig. 4. Optimization of Ar flow rate for: A—As 228.812 nm (50 ng ml^{-1}); B—Sb 259.805 nm (10 ng ml^{-1}). Plasma power: 25 W. Error bars correspond to the standard deviation for 5 independent measurements.

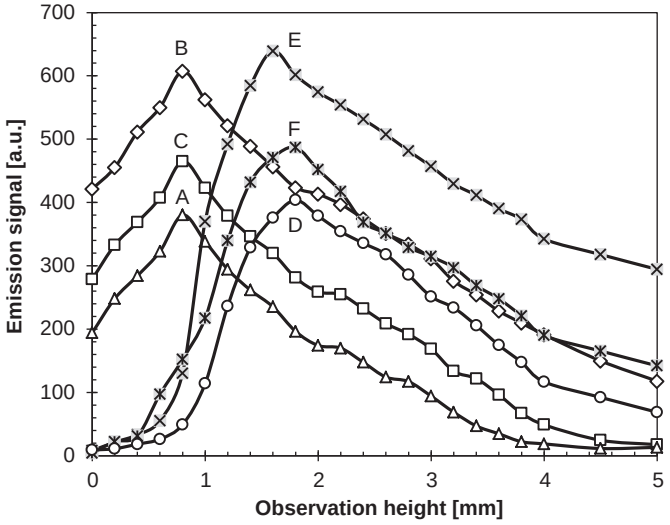

Fig. 5. Emission signal *vs.* viewing height and different plasma power levels for As 228.812 nm (50 ng ml^{-1}) (curves A–C) and Sb 259.805 nm (10 ng ml^{-1}) (curves D–F). Power (W): A, D–20; B, E–25; C, F–30. Ar flow rate: 0.4 l min^{-1}.

flow rate for a plasma power of 25 W. A flow rate of 0.4 l min^{-1} Ar for hydride transport and plasma operation was retained as optimal for both elements.

Fig. 5 shows the variation of the emission signal with observation height for different plasma power levels and an Ar flow rate of 0.4 l min^{-1}.

For both elements, the optimal operation power of plasma was 25 W. The influence of observation height as a critical variable on sensitivity was rigorously investigated, and the optimal values for 25 W plasma power were 0.8 mm (As) and 1.6 mm (Sb) above the tip microelectrode. Although hydride generation from As(III) and Sb(III) occurred under similar experimental conditions, the simultaneous determination by HG-μCCP-OES was not possible given the significant difference between the optimum viewing heights for the two elements.

3.3. Figures of merit

The characteristics of calibration curves and detection limits in HG-μCCP-OES according to the 3σ criterion (3Sb/m) are given in Table 2. The standard deviation of the background (Sb) was found from 10 independent measurements of the blank calibration solution in the proximity of the spectral lines.

The analytical sensitivity and detection limit of Sb were 5.3 and 4.7 times better, respectively, than those for As. Defining the limit of quantification as the analyte concentration required to produce a net signal 10-times greater than the background standard deviation, HG-μCCP-OES allowed the accurate quantitation of at least 1.5 mg kg^{-1} As and 0.3 mg kg^{-1} Sb in plastics and biodegradable materials with a precision of at least 10%. Table 3 compares the detection limits obtained by HG-μCCP-OES and other techniques used in the analysis of plastics or other samples.

According to the data in Table 3, the detection limit of Sb by HG-μCCP-OES is better than by ICP-OES and FAAS without derivatization. The antimony detection limit in plastics is also better than that obtained by slurry sampling GFAAS. However, the detection limits in HG-μCCP-OES of both As and Sb are poorer than those reported in plastic materials by ICP-MS, which is recognized for its remarkable sensitivity. Despite the analytical performance of ICP-OES, HG-ICP-OES, ICP-MS and HG-ICP-MS, the HG-μCCP-OES system is advantageous because the acquisition cost of ICP equipment is much higher than that of a microspectrometer interfaced with a microtorch.

The detection limits of As and Sb in HG-μCCP-OES are poorer or similar to those obtained by Ar-hydrogen cold flame atomic fluorescence spectrometry, which is recognized for its exceptional analytical potential for hydride-forming elements due to its very low background. The detection limits for HG-μCCP-OES are poorer than those for HG-AAS with As and Sb hydride preconcentration on tungsten coil, quartz tube or platform.

The sensitivity of HG-μCCP-OES is better than that reported for non-conventional analytical systems using microplasma sources (HG-MSP-OES, HG-DBD-AAS) operated at lower power than our source. The cause of this difference is the negative effect of the presence of hydrogen and water vapor on the discharge stability and the lower atomization/excitation capability of microwave

Table 2
Characteristics of the calibration curves and limits of detection by HG-μCCP-OES.

Element	λ (nm)	Calibration range (ng ml^{-1})	Slope (m) (a.u. ml ng^{-1})	RSD slope (%)	Correlation coefficient (r)	LOD	
						(ng ml^{-1})	(mg kg^{-1})
As	228.812	5–100	12.2	0.7	0.9999	1.4	0.5[a]
Sb	259.805	1–100	64.0	0.3	0.9995	0.3	0.1[a]

[a] Calculated for 150 mg sample dissolved in 50 ml solution.

Table 3
Limits of detection of As and Sb by HG-μCCP-OES compared to those of other analytical systems.

Method	Sample	LOD As		LOD Sb		Reference
		(ng ml^{-1})	(mg kg^{-1})	(ng ml^{-1})	(mg kg^{-1})	
HG-μCCP-OES	Plastics and biodegradable materials	1.4	0.5[a]	0.3	0.1[a]	This paper
ICP-OES	Polymers	–	–	–	48	[9]
FAAS	Polymers	–	–	–	290	[9]
EDXRF	Polymers	–	–	–	7.9	[9]
ICP-MS	Plastic food packaging	–	0.000117	–	0.000010	[10]
FAAS/bromide vapor	PET	–	–	–	1.39	[11]
GFAAS slurry	Plastics	–	–	6.8	–	[12]
GFAAS solid sampling	Soil/airborne particulate matter	–	0.5	–	0.1/15	[36,37]
HG-ICP-OES	Drinking water	0.7	–	2.1	–	[21]
HG-ICP-MS	Water		–	0.017	–	[22]
HG-AAS without trapping	Water	0.25	–	–	–	[19]
	Soil	0.1	0.04	–	–	[31,35]
HG-AAS trapping	Water	–	–	0.016/0.013	–	[18,20]
HG-AFS	River water	0.37	–	0.32	–	[23]
	TCM	0.034	–	0.027	–	[24]
HG-AFS trapping	Natural water	0.010	–	–	–	[25]
HG-MSP-OES	Coal fly ash	18/6	–	31/7	–	[26. 27]
HG-DBD-AAS	Orchard leaves, urine	1	–	–	–	[28]
	Water	–	–	13	–	[29]
HG-DBD-AFS	Vegetable	–	–	0.11	–	[30]

[a] Calculated for 150 mg sample dissolved in 50 ml solution.

Table 4
Average As and Sb (mg kg^{-1}) and expanded uncertainty in polyethylene certified reference materials by HG-μCCP-OES.

Element	ERM EC 680k		ERM EC 681k	
	Certified	Found[a]	Certified	Found[a]
As	4.1 ± 0.5	4.2 ± 0.2	29.1 ± 1.8	29.1 ± 0.2
Sb	10.1 ± 1.6	10.0 ± 0.2	99 ± 6	99 ± 1

[a] Expanded uncertainty for 95% confidence level and $n=5$ independent measurements.

Table 5
As and Sb determination ($n=5$) by HG-μCCP-OES in non- and biodegradable materials.

Materials	Sample size	As				Sb			
		Content (mg kg^{-1})			s_r (%)[a]	Content (mg kg^{-1})			s_r (%)[a]
		Min	Max	Average		Min	Max	Average	
ABS[b]	10	23.9	46.2	31.4	0.4–4.0	15.7	156	49.3	0.4–3.2
PE[c] shopping bag	10	10.2	20.5	15.9	3.3–5.5	7.1	22.3	16.4	0.5–2.8
Biodegradable materials[d]	10	11.2	18.9	15.7	1.7–7.1	12.5	17.7	15.2	0.7–1.8
PET[e] still/mineral water	10	23.8	35.0	28.9	1.1–4.0	45.1	63.7	55.0	0.7–2.1

[a] Relative standard deviation of repeatability ($n=5$).
[b] Acrylonitrile butadiene styrene from personal computers.
[c] Polyethylene.
[d] Shopping bags of (oxo-)biodegradable polyethylene (OPE) or corn starch.
[e] Bottles of polyethylene terephthalate.

microplasmas. For such systems, the detection limits improve significantly when using electrochemical hydride generation instead of a chemical procedure due to the lower amount of hydrogen generated and introduced into the plasma [27].

3.4. Sample analysis

Table 4 presents the results obtained for the determination of As and Sb in two polyethylene certified reference materials with low and high hazardous element contents.

According to the data in Table 4, HG-μCCP-OES provided reliable results for As and Sb determination in plastic materials, with recoveries of 101 ± 2% (As) and 100 ± 1% (Sb) within a 95% confidence level. This excellent recovery is due to the efficient release of analytes following the oxidation of the organic matrix by acidic microwave digestion in a nitric–sulfuric acid mixture, which enabled the external calibration approach. The results obtained for As and Sb determination in real non- and biodegradable material samples are presented in Table 5.

For 10.2–46.2 mg kg^{-1} As and 7.1–156 mg kg^{-1} Sb, the overall precision of the proposed method was 0.4–7.1% and 0.4–3.2%, respectively. Arsenic and Sb concentrations were higher in non-biodegradable materials: As was highest in ABS and PET, whereas Sb in ABS. Neither element exhibited a significant difference in content in PE, OPE and corn starch used for packaging. Although adequate recycling programs already exist for electronic equipment, small packaging is often disposed of in the refuse bin as regular household waste. This type of waste is a possible environmental contamination risk with respect to As and Sb given the high degradation rate of biomaterials.

4. Conclusions

The proposed method for As and Sb determination using the HG-μCCP-OES miniature analytical system with an Ar capacitively coupled plasma microtorch as the novelty element was successfully applied to analyze recycling plastics and biodegradable materials. Monitoring As and Sb in such materials is necessary because of the toxicity of these elements, despite their omission from the scope of RoHS. The use of L-cysteine allowed the pre-reduction of As and Sb and subsequent hydride generation with $NaBH_4$ in very low dilute HCl solution under the same chemical conditions. However, measurements were performed sequentially because of the significant difference between the optimum observation heights in plasma for the two elements. The analytical system is viable as laboratory equipment, and the use of the derivatization approach provides sensitivity comparable with conventional systems based on ICP-OES and FAAS with/without derivatization. Another benefit of the method based on the HG-μCCP-OES analytical system is the lower analysis cost due to the low consumptions of power, Ar to sustain plasma and high-purity hydrochloric acid.

Acknowledgments

This work was supported by a grant of the Romanian National Authority for Scientific Research, CNDI–UEFISCDI, project number PN-II-PT-PCCA-2011-3.2-0219 (Contract no. 176/2012)

References

[1] C.O. Abernathy, Y.P. Liu, D. Longfellow, H.V. Aposhian, B. Beck, B. Fowler, R. Goyer, R. Menzer, T. Rossaman, C. Thompson, M. Waalkes, Environ. Health Perspect. 107 (1999) 593–597.
[2] International agency for Research on Cancer, Summary and Evaluations, 〈http://www.inchem.org/documents/iarc/vol47/47-11〉. html (accessed in 01 August 2012).
[3] U.S. Environmental Protection Agency, Integrated Risk Information System (IRIS) on Antimony, National Center for Environmental Assessment, Office of Research and Development, Washington, DC, 1999.
[4] Deutsche Forschungsgemeinschaft (DFG) Analysis of Hazardous Substances in Biological Materials, VCH, Weinheim, 1994.
[5] F. Welle, R. Franz, Food Addit. Contam. A 28 (2011) 115–126.
[6] M. Krachler, W. Shotyk, Sci. Total Environ. 407 (2009) 1089–1096.
[7] W. Shotyk, M. Krachler, Environ. Sci. Technol. 41 (2007) 1560–1563.

[8] M. Ristic, I. Popovic, V. Pocajt, D. Antanasijevic, A. Peric-Grujic, Food Addit. Contam. B 4 (2011) 6–14.
[9] E. Dimitrakakis, A. Janz, B. Bilitewski, E. Gidarakos, Waste. Manage. 29 (2009) 2700–2706.
[10] E. Skrzydlewska, M. Balcerzak, Chem. Anal. 48 (2003) 909–918.
[11] A. Lopez-Molinero, P. Calatayud, D. Sipiera, R. Falcon, D. Liñan, J.R. Castillo, Microchim. Acta 158 (2007) 247–253.
[12] M.C. Santos, J.A. Nóbrega, N. Baccan, S. Cadore, Talanta 81 (2010) 1781–1787.
[13] A.R. Kumar, P. Riyazuddin, Int. J. Environ. Anal. Chem. 87 (2007) 469–500.
[14] M.A. Vieira, P. Grinberg, C.R.R. Bobeda, M.N.M. Reyes, R.C. Campos, Spectrochim. Acta, Part B 64 (2009) 459–476.
[15] M. Krachler, H. Emons, J. Zheng, TrAC, Trends Anal. Chem. 20 (2001) 79–90.
[16] P. Smichowski, Talanta 75 (2008) 2–14.
[17] Y.W. Chen, N. Belzile, Anal. Chim. Acta 671 (2010) 9–26.
[18] S. Titretir, E. Kendüzler, Y. Arslan, I. Kula, S. Bakirdere, O.Y. Ataman, Spectrochim. Acta, Part B 63 (2008) 875–879.
[19] A.R. Kumar, P. Riyazuddin, Int. J. Environ. Anal. Chem. 88 (2008) 255–266.
[20] J. Kratzer, J. Dědina, Spectrochim. Acta, Part B 63 (2008) 843–849.
[21] A. Tyburska, K. Jankowski, A. Ramsza, E. Reszke, M. Strzelec, A. Andrzejczuk, J. Anal. At. Spectrom. 25 (2010) 210–214.
[22] Y.-L. Feng, H. Narasaki, L.-C. Tian, H.-Y. Chen, At. Spectrosc. 21 (2000) 30–36.
[23] W.-B. Zhang, X.-A. Yang, Y.-P. Dong, X.-F. Chu, Spectrochim. Acta, Part B 65 (2010) 571–578.
[24] W.-B. Zhang, X.-A. Yang, X.-F. Chu, Microc. J. 93 (2009) 180–187.
[25] R. Liu, P. Wu, M. Xi, K. Xu, Y. Lv, Talanta 78 (2009) 885–890.
[26] P. Pohl, I.J. Zapata, N.H. Bings, E. Voges, J.A.C. Broekaert, Spectrochim. Acta, Part B 62 (2007) 444–453.
[27] P. Pohl, I.J. Zapata, N.H. Bings, Anal. Chim. Acta 606 (2008) 9–18.
[28] Z. Zhu, S. Zhang, Y. Lv, X. Zhang, Anal. Chem. 78 (2006) 865–872.
[29] Z. Zhu, S. Zhang, J. Xue, X. Zhang, Spectrochim. Acta, Part B 61 (2006) 916–921.
[30] Z. Zhu, J. Liu, S. Zhang, X. Na, X. Zhang, Spectrochim. Acta, Part B 63 (2008) 431–436.
[31] E.A. Cordos, T. Frentiu, M. Ponta, I. Marginean, B. Abraham, C. Roman, Chem. Speciation Bioavailability 18 (2006) 11–25.
[32] T. Frentiu, D. Petreus, M. Senila, A.I. Mihaltan, E. Darvasi, M. Ponta, E. Plaian, E.A. Cordos, Microc. J. 97 (2011) 188–195.
[33] T. Frentiu, A.I. Mihaltan, M. Ponta, E. Darvasi, M. Frentiu, E. Cordos, J. Hazard. Mater. 193 (2011) 65–69.
[34] T. Frentiu, A.I. Mihaltan, E. Darvasi, M. Ponta, C. Roman, M. Frentiu, J. Anal. At. Spectrom. 27 (2012) 1753–1760.
[35] E.A. Cordos, T. Frentiu, M. Ponta, B. Abraham, I. Marginean, Chem. Speciation Bioavailability 18 (2006) 1–9.
[36] P. Török, M. Žemberyová, Spectrochim. Acta, Part B 65 (2010) 291–296.
[37] R.G.O. Araujo, B. Welz, I.N.B. Castilho, M.G.R. Vale, P. Smichowski, S.L.C. Ferreira, H. Becker-Ross, J. Anal. At. Spectrom. 25 (2010) 580–584.